

# Advanced Techniques for Nanocharacterization Of Polymeric Coating Surfaces

Xiaohong Gu<sup>†</sup>, Tinh Nguyen, Li-Piin Sung, Mark R. VanLandingham,<sup>\*\*</sup> Michael J. Fasolka, and Jonathan W. Martin—National Institute of Standards and Technology\*

Y.C. Jean—University of Missouri—Kansas City<sup>†</sup>

Diep Nguyen—PPG Industries, Inc.<sup>‡</sup>

Nei-Kai Chang and Tsun-Yen Wu—National Taiwan University<sup>\*\*\*</sup>

*Surface properties of a polymeric coating system have a strong influence on its performance and service life. However, the surface of a polymer coating may have different chemical, physical, and mechanical properties from the bulk. In order to monitor the coating property changes with environmental exposures from the early stages of degradation, nondestructive techniques with the ability to characterize surface properties with micro- to nanoscale spatial resolution are required. In this article, atomic force microscopy has been applied to study surface microstructure and morphological changes during degradation in polymer coatings. Additionally, the use of AFM with a controlled tip-sample environment to study nanochemical heterogeneity and the application of nanoindentation to characterize mechanical properties of coatings surfaces are demonstrated. The results obtained from these nanometer characterization techniques will provide a better understanding of the degradation mechanisms and a fundamental basis for predicting the service life of polymer coatings.*

*Keywords: Atomic force, surface analysis, interface analysis, epoxy resins, fluorinated polymers, hardness, scratch resistance, service life prediction, surface chemistry, morphology*

Polymeric coatings are widely used in buildings, bridges, automobiles, and electronic equipment for both functional and aesthetic purposes. Despite great improvements in coatings technology, problems still exist in the long-term performance of polymeric coatings exposed to environments such as ultraviolet light, humidity, temperature, and other aggressive conditions. Generally, the surface properties of a coating system have a strong influence on its performance and service life. These properties include surface morphology and microstructure, surface chemistry, optical appearance, and surface mechanical properties such as hardness, modulus, and scratch resistance. Application-specific performance requirements often create complicated interactions between these properties that are important to quantify as a function of service conditions. However, the surface of a polymeric coating system may have different chemical, physical, and mechanical properties from the bulk.<sup>1,2</sup> For example, the concentration of low surface-energy materials is often higher at the air surface than in the bulk,<sup>3,4</sup>

especially in a multicomponent coating system. Thus, characterization of bulk material properties might not be sufficient for predicting performance. Techniques with sensitivity to the surface chemical, physical, and mechanical properties are required.

An additional factor that complicates the prediction of coating performance and service life is that polymer coatings are heterogeneous<sup>5,6</sup> and contain nano- to micrometer scale degradation-susceptible regions. Degradation of a polymer coating is believed to start from these degradation-susceptible regions on the surface and then grow laterally and vertically. In the early stages of degradation, even though obvious chemical changes have been observed, the physical changes of the coating surface could still be small,<sup>7</sup> so that degraded regions such as pits may have dimensions that are on the order of nanometers in depth and perhaps tens or a few hundreds of nanometers in width. As exposure time increases, a more significant morphological evolution is generally observed on the sample surface; however, significant changes in mechani-

*Presented at the 81st Annual Meeting of the Federation of Societies for Coatings Technology on November 12-14, 2003, in Philadelphia, PA.*

\* Gaithersburg, MD 20899.

† Kansas City, MO 64110.

\*\* Current affiliation: Army Research Laboratory, Aberdeen Proving Ground, MD 21005.

‡ Allison Park, PA 15101.

\*\*\* Department of Mechanical Engineering, Taipei, Taiwan.

cal performance or appearance may not be detected using conventional testing until the degradation has progressed to an advanced state.<sup>8</sup> In order to monitor the coating property changes with exposure from the early stages of degradation, nondestructive techniques with the ability to characterize surface properties with micro- to nanoscale spatial or depth resolution are required. Information obtained from such characterization can then be used to provide a more complete understanding of degradation mechanisms, providing a fundamental basis for predicting the service life of polymer coatings.

Tapping mode atomic force microscopy (AFM) has emerged as a powerful technique to provide direct spatial mapping of surface topography and surface heterogeneity

with nanometer resolution. Phase contrast in tapping mode AFM often reflects differences in the properties of individual components of heterogeneous materials, and is useful for compositional mapping in polymer blends, copolymers, and coatings.<sup>9-15</sup> Additionally, force curves in tapping mode AFM have also been explored to provide local mechanical property information in multicomponent materials.<sup>16</sup> A combination of phase imaging and force curve measurement can allow the heterogeneous regions in polymer systems to be identified. Development of chemical modification of AFM probes has demonstrated that chemical sensitivity of AFM can be enhanced by functionalizing tips with specific chemical species<sup>17,18</sup> or by elevating the humidity of the tip-sample environment.<sup>19,20</sup> This capability allows AFM to be used to image surface morphology and surface heterogeneity based on local chemical interactions, making the linkage between physical properties and chemical properties possible at micro- to nanometer scales.

Nanoindentation has been increasingly used to characterize the mechanical response of polymer materials.<sup>8,21-23</sup> This technique is characterized relative to traditional indentation techniques by the small radius of the indentation probes, the continuous and simultaneous measurement of forces and displacements, the extremely high force and displacement resolutions, and the large ranges of applied forces and displacements. These capabilities allow for the study of a variety of materials with micrometer and submicrometer scale resolution, both in lateral dimension and in penetration depth. The addition of dynamic oscillation superposed over a quasi-static loading history allows for the characterization of mechanical properties as a function of penetration depth as opposed to a single measurement from the quasi-static loading history. The dynamic capability can also be used to measure mechanical storage and loss and other time-dependent behavior of polymers, such as creep and stress relaxation. Lateral motion and lateral force measurement capabilities have also been developed to extend the nanoindentation instrument to surface tribological studies, such as scratch resistance of coatings.

In this article, AFM and nanoindentation techniques are applied to study surface microstructure, properties, and degradation of polymer coatings. Tapping mode AFM

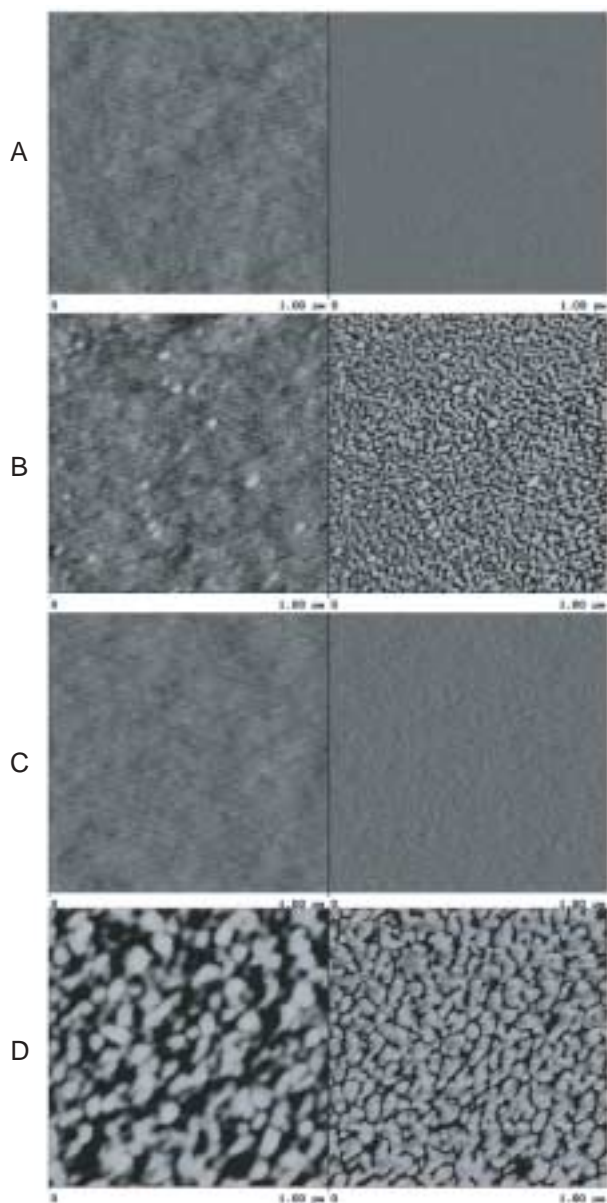


Figure 1—AFM height images (left) and phase images (right) of epoxy coatings applied on silicon substrates: (A) E1000, surface; (B) E1000, interface; (C) E2575, surface; (D) E2575, interface. Scan size is  $1 \times 1 \mu\text{m}$ . Contrast variations from white to black are 10 nm for the height images and  $90^\circ$  for the phase images.

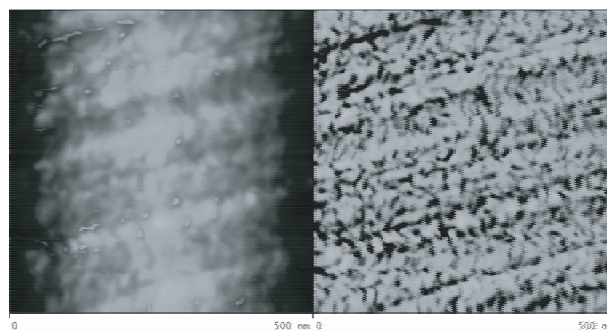


Figure 2—AFM height image (left) and phase image (right) of ultramicrotomed fractured surface of epoxy E1000 bulk specimen. Scan size is  $500 \times 500 \text{ nm}$ . Contrast variations from white to black are 10 nm for the height images and  $30^\circ$  for the phase images.

is used to investigate changes in surface microstructure as a function of exposure. Additionally, the use of AFM with a controlled tip-sample environment to image chemical heterogeneity in coating surfaces and the application of nanoindentation to studies of surface mechanical properties, such as modulus, hardness, and scratch resistance are demonstrated.

## EXPERIMENTAL PROCEDURES\*

### Materials and Sample Preparation

The surfaces and interfaces of several polymer film samples were studied as a function of exposure to a particular environment. Epoxy samples were prepared using a highly pure diglycidyl ether of bisphenol A (DGEBA) with an epoxy equivalent of 172 g/equiv. The curing agents used were mixtures of 1,3-bis(aminomethyl)-cyclohexane (BAC) and cyclohexylmethylamine (CMA). Samples of four different crosslinked epoxies were prepared with stoichiometric blends of DGEBA with appropriate amine mixtures. The molar ratios for BAC and CMA were 100/0, 75/25, 50/50, and 25/75 for samples identified as E1000, E7525, E5050, and E2575, respectively. Films with an approximate thickness of 300  $\mu\text{m}$  were prepared in a  $\text{CO}_2$ -free and  $\text{H}_2\text{O}$ -free glove box by a drawdown technique. All samples were cured at room temperature for 24–48 hr, followed by post-curing at 130°C for two hours. The coated films were removed from the silicon substrates by cooling in liquid nitrogen, followed by peeling with tweezers. The film side in contact with the silicon substrate is the interface side, while the side exposed to air is the surface side. Surface morphology and surface mechanical properties of epoxy samples were studied by AFM, nanoindentation, and other techniques during exposure to outdoor environments in the Washington D.C. area.

Blend films of poly(vinylidene fluoride) (PVDF) and a copolymer of poly(methyl methacrylate) (PMMA) and poly(ethyl acrylate) (PEA) were prepared by mixing a PVDF-isophorone suspension with solutions of PMMA-co-PEA in toluene. The mass ratios between PVDF and PMMA-co-PEA were 70/30, 60/40, 50/50, and 30/70. The mixtures were cast on glass plates by drawdown to provide a 75- $\mu\text{m}$  thick film. After heating at 246°C for 10 min in an air-circulated oven, coated glass plates were removed from the oven and slowly cooled to ambient temperature (24°C). After being immersed in boiling water for 10 min, the films were readily peeled from the glass plates. Again, the film side exposed to the air during film formation is the surface side and the side in contact with the glass substrate is the interface side. Surface and interface morphology was characterized by AFM before and after exposure to UV light at 50°C and 9% relative humidity (RH) for seven months. The radiation source of UV light was supplied by a 1000 W xenon arc solar simulator, which provided infrared-free, near ambient

temperature (24°C) radiation with wavelengths between 275 and 800 nm.

Polyester-free films with an approximate thickness of 670  $\mu\text{m}$  were studied using AFM as a function of exposure to a 3 mol/l NaOH solution. The samples were prepared by mixing 100 parts of an isophthalate ester resin and two parts of methyl ketone peroxide catalyst. The mixture was then molded between two sealed acrylic plates. Then the samples were cured in ambient condition overnight followed by post-curing at 150°C for two hours in an oven.

Two types of chemically heterogeneous polymer samples were studied using AFM with an environmental chamber. The first sample was a block polymer of polystyrene-b-polyethylene (PS-b-PEO). The bulk specimen of PS-b-PEO was annealed at 180°C and then fractured under liquid nitrogen. The fractured surface was examined using AFM in tapping mode under different RH levels. A second polymer specimen was a bilayer of PS and poly(acrylic acid) (PAA). The PS-PAA sample was prepared by

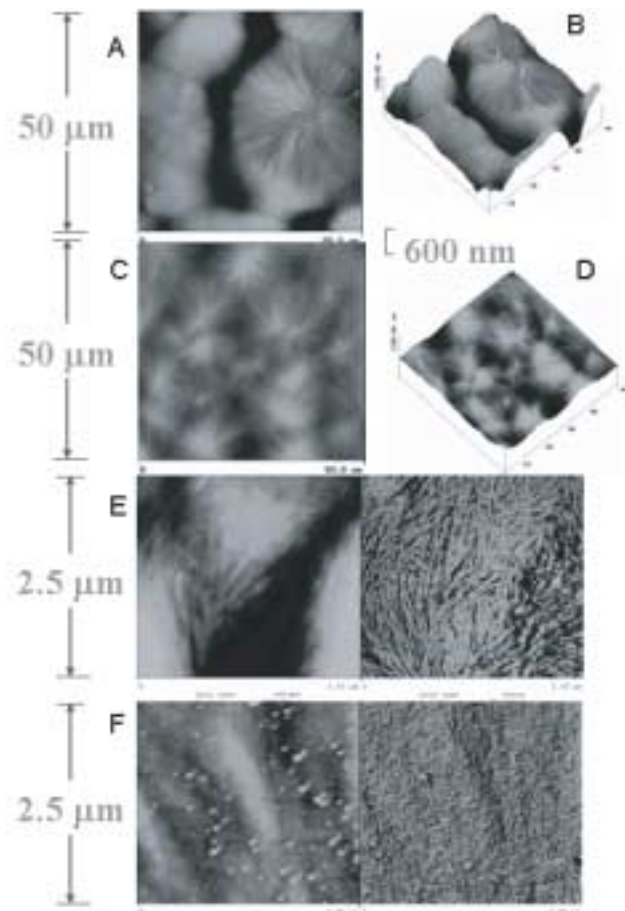


Figure 3—AFM images of a 70/30 PVDF/PMMA-co-PEA blend film: (A) and (B) are 2D and 3D height images of the surface side, respectively; (C) and (D) are 2D and 3D height images of the interface side, respectively. The scan size is 50  $\times$  50  $\mu\text{m}$  for A–D. Contrast variations from black to white are 1200 nm for (A) and 500 nm for (C). (E) and (F) are topographic and phase images of the surface side and the interface side of the blend film, respectively. The scan size is 2.5  $\times$  2.5  $\mu\text{m}$ . Contrast variations from black to white are 50 nm for the height image and 90° for the phase image.

\*Certain commercial products or equipment are identified so as to specify adequately the experimental procedure. In no case does such identification imply recommendation or endorsement by NIST, nor does it imply that it is necessarily the best available for the purpose.

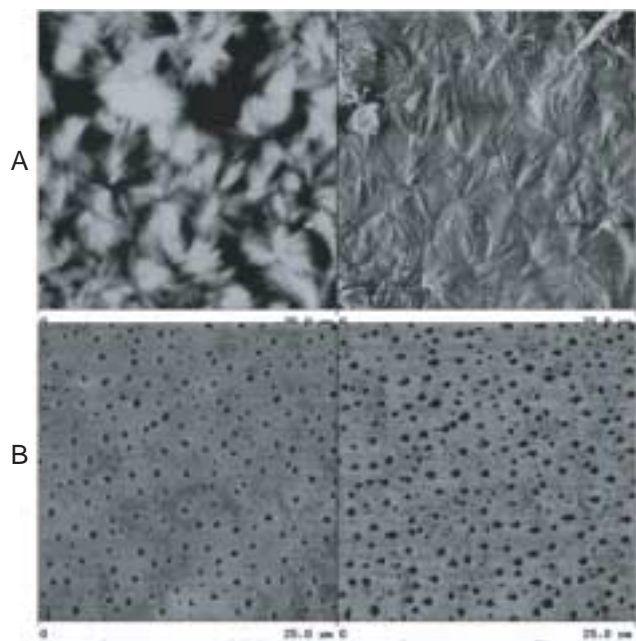


Figure 4—AFM height (left) and phase (right) images of the 50/50 PVDF/PMMA-co-PEA blend film: (a) Surface; the scan size is  $2.5 \times 2.5 \mu\text{m}$ ; contrast variations from black to white are 50 nm for the height image and  $25^\circ$  for the phase image; (b) Interface; the scan size is  $7.5 \times 7.5 \mu\text{m}$ ; contrast variations from black to white are 50 nm for the height image and  $30^\circ$  for the phase image.

spin casting a PS solution in toluene onto the silicon substrate, and then a solution of PAA in water was spuncast onto the PS layer. Due to the low surface energy of PS, the PAA dewetted over the PS layer thus forming viscous fingering patterns.<sup>24</sup>

PMMA and the high crystalline polypropylene (PP) that were studied using instrumented indentation and scratch testing were commercial products. Other materials and their preparation procedures and degradation conditions will be described individually in the article.

### Atomic Force Microscopy

Tapping mode AFM was used to characterize the epoxy, PVDF/PMMA-co-PEA, and polyester films as a function of exposure to various environments. A Digital Instruments Dimension 3100 AFM with a NanoScope 3a controller (Veeco Metrology) was operated in tapping mode under ambient conditions. Additionally, PS-b-PEO and PS-PAA samples were studied with the same AFM but used a small volume environmental chamber to control the RH of the imaging environment over a range of nominally 0–95% RH.<sup>20</sup> Commercial silicon microcantilever probes were used that had manufacturer's values of probe tip radius and probe spring constant in the ranges of 5–10 nm and 20–100 N/m, respectively. Topographic and phase images were obtained simultaneously using a resonance frequency of approximately 300 kHz for the probe oscillation and a free-oscillation amplitude of  $60 \pm 5$  nm. A set-point ratio ( $r_{sp}$ ) in the range of 0.70–0.90 was used. To obtain the mechanical response of different domains in some of the films, force curves were performed utilizing the same type of silicon cantilever described previously. While more in-

depth analysis of the force curves can be used to measure relative modulus values, the identity of mechanically different regions can be inferred simply from the slope and shape of the repulsive or contact portion of the force curve.<sup>16</sup>

### Nanoindentation and Scratch Testing

Nanoindentation was performed using Nanoindenter XP and Nanoindenter DCM (MTS System, Inc). The nanoindenter was operated using the continuous stiffness method with a Berkovich indenter. The tip shape of the indenter was directly imaged with AFM.<sup>25</sup> Ten to 20 indents were made on each sample, from which averages of modulus and hardness were calculated. The scratch tests on E1000, PMMA, and high crystalline PP were performed using the Nanoindenter XP with a  $1\text{-}\mu\text{m}$ -radius  $90^\circ$ -conical diamond tip by constant-load and progressive-load scratch test methods. Scratch velocity was held constant through each scratch test and could be set from  $0.05 \mu\text{m/s}$  to  $2.5 \text{ mm/s}$ . The scratch deformation patterns were examined by laser scanning confocal microscopy.

## RESULTS

### Imaging Surface Microstructure of Coatings with AFM

The advantage of tapping mode AFM for studying coating surface microstructure is its ability to provide direct spatial mapping of surface topography and surface heterogeneity with nanometer resolution. Surface topographic maps are generated through signal feedback in which the tapping amplitude is maintained at a constant. Any changes in the oscillation phase can be used to provide phase contrast, which often reflects the different mechanical, chemical, and/or adhesive properties of the different phases or components of heterogeneous materials, thus mapping heterogeneity.

Examples of the use of topographic (height) and phase contrast images to study the microstructure of surface and interface sides of two different crosslinked epoxies are shown in *Figure 1*. For both the highly crosslinked E1000 ( $M_c = 364 \pm 16 \text{ g/mol}$ ) sample and the lower crosslinked E2575 ( $M_c = 1950 \pm 188 \text{ g/mol}$ ) sample, the height and phase images of the interface side exhibit more contrast as compared to those of the surface side. The interface side is considerably rougher than the surface side, showing well-defined nodular structures. It should be mentioned that the silicon surface is essentially smooth and featureless, as observed in AFM images with the same magnification.

The two-phase microstructure, consisting of a light matrix and relatively dark interstitial regions, indicates that the interface side of epoxy is heterogeneous. This microstructure is similar to that obtained from the ultramicrotomed fractured surface of an E1000 bulk sample, shown in *Figure 2*; though the nodules of the bulk sample are slightly smaller and not as organized as those on the interface side (see *Figure 1B*). Such a heterogeneous structure is confirmed further with the microstructure of the degraded sample, which will be shown later. In contrast, the surface sides appear homogeneous with smooth to-

pography and little phase contrast. Such morphological differences between the surface and interface or the bulk have also been observed for acrylic melamine and other epoxies in our laboratory.<sup>26</sup> Further, one can find that the crosslink density has an obvious influence on the microstructure of the interface, though no significant effects on the surface. The size of the bright nodules in the phase image of the interface is larger for the lower crosslinked E2575 sample compared to the highly crosslinked E1000 sample, while the surface sides for both are featureless. We believe that such differences are due to the surface enrichment of the low surface energy species at the air-film surface and to the preferential absorption and interaction of high polarity materials in the interface region. The polarity results obtained from our contact angle measurements have provided evidence for such a hypothesis. For each epoxy, the polarity of the interface is higher than that of the surface, indicating that the air surface of these types of coatings could be dominated by a thin layer of lower surface energy materials or groups. Additionally, the surface polarity appears independent of network vari-

ation while the interface polarity increases with decreasing crosslinking.<sup>27</sup>

For a multicomponent polymer coating system, such as PVDF/PMMA-co-PEA blends, the morphological difference between the surface side and the interface side is significant. AFM images provide not only morphological information but also reveal the fine microstructure of the PVDF crystallites. In Figure 3, two-dimensional (A,C) and three-dimensional (B,D) AFM topographic images are shown of the surface and the interface of a 70/30 PVDF/PMMA-co-PEA blend film at a scan size of  $50 \times 50 \mu\text{m}$ . The spherulites at the surface and the interface differ significantly in their sizes, shapes, and distribution density. The large and circular crystallites in A and B almost cover the surface completely, while the crystallites at the interface are loosely packed and less impinged. The interface is also smoother than the surface due to the smaller diameter of the crystallites.

At a smaller scan size of  $2.5 \mu\text{m}$  (Figures 3E and 3F), the lamellar structure is clearly observed in the spherulites at the surface side. On the other hand, at the interface side, particles are observed on the spherulites or aggregate in

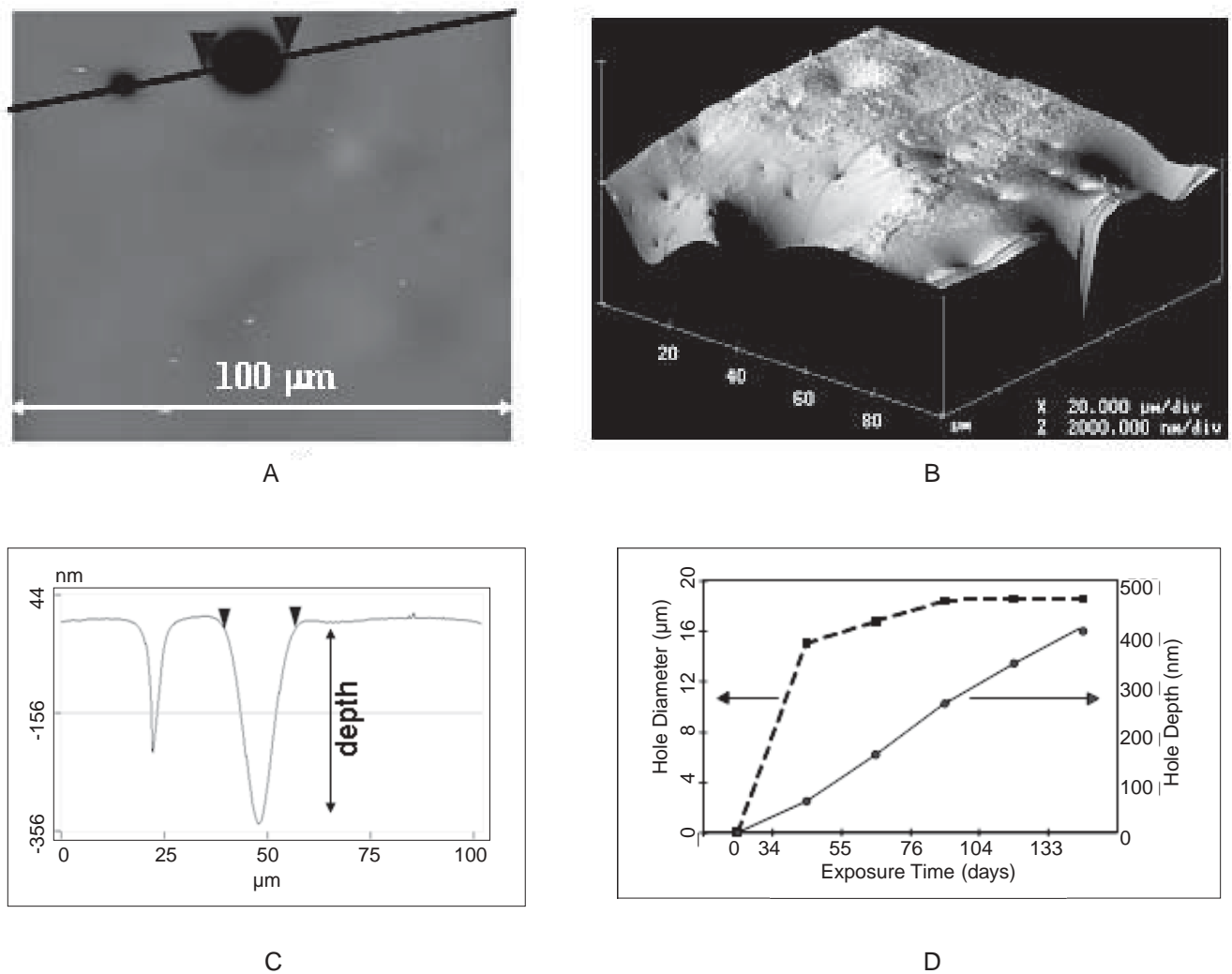


Figure 5—Monitoring pit evolution by AFM for a clear acrylic-urethane coating exposed to a xenon arc lamp for 6160 hr at  $50^\circ\text{C}/70\% \text{RH}$ ; (A) 2D image with a line crossing two pits, (B) 3D image, (C) profile corresponding to line in (A) showing pit width and depth, and (D) depth and diameter of the large pit as function of exposure time.

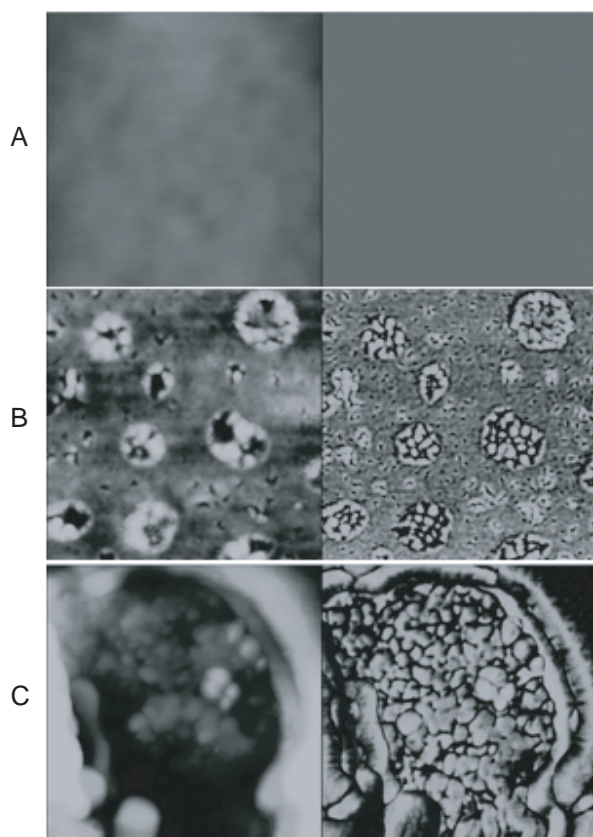


Figure 6—AFM height (left) and phase (right) images of an epoxy (E1000) film exposed to an outdoor environment during the summer in the Washington D.C. area: (A) before exposure; (B) after exposure for one month; (C) after exposure for two months. The scan sizes are  $1 \times 1 \mu\text{m}$ . Contrast variations from black to white are 30 nm for height images and  $60^\circ$  for phase images.

the boundaries between crystallites. We believe that these particles are mainly PMMA-co-PEA, because these amorphous materials tend to be rejected into the interlamellae regions or the fronts of the spherulites during PVDF crystallization.<sup>28,29</sup> The above observations indicate that the composition, the crystallinity, and/or the crystallization kinetics might be different between the surface and the interface of the blend film. Attenuated total reflection Fourier-transform infrared (ATR-FTIR) spectra and surface free energy results have confirmed that the air surface of the blend film is enriched with the low surface-free energy PVDF, and the interface side contains more polar acrylic copolymers.<sup>30</sup> With increasing PMMA-co-PEA in the blend, the morphological and microstructural differences are more evident between the two sides, as shown in Figure 4. The surface of the 50/50 PVDF/PMMA-co-PEA blend film is mostly covered with spherulites, but the interface side consists of many holes surrounded by smooth areas. Similarly, it has been demonstrated using ATR-FTIR and other techniques that PVDF enriches the air surface of the film, while the amorphous PMMA-co-PEA component dominates the polymer/substrate interface. Such morphological and compositional differences are believed to strongly affect the performances of these coating systems.

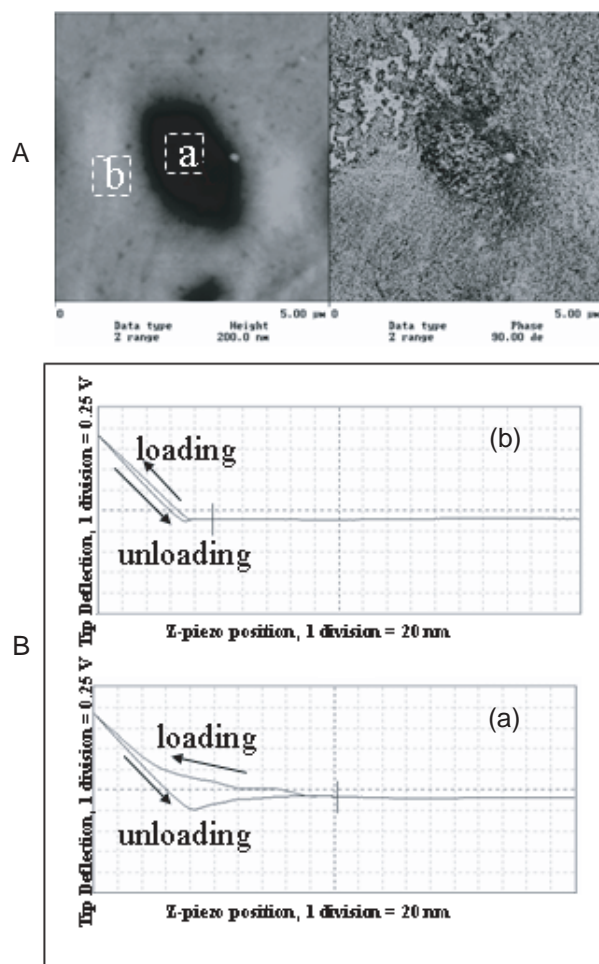


Figure 7—(A) AFM height (left) and phase (right) images of an area around a pit in the polyester film exposed to 3 mol/l NaOH environment for 28 days. The scan size is  $5 \times 5 \mu\text{m}$ . Contrast variations from black to white are 200 nm for the height image and  $90^\circ$  for the phase image. (B) Typical force curves for (a) a dark region inside the pit and (b) a bright region outside the pit. The positions of (a) and (b) are shown in (A).

### Monitoring Surface Degradation Using AFM

One particular advantage to using AFM for studying the degradation of polymer coatings is its capability to image the surface change of the same location of coatings as a function of exposure with nanometer resolution. One example is using AFM to monitor the formation and evolution of pits on the surface of an acrylic-urethane coating film with exposure to a xenon arc lamp at 70% RH and  $50^\circ\text{C}$  (Figure 5). The sample was approximately 10- $\mu\text{m}$  thick and was applied onto a  $\text{CaF}_2$  substrate by spin-coating. At the early stage of degradation, the highlighted pit is only a few nanometers deep and wide. With the increase of the exposure time, the pit depth has a nearly linear increase, up to 400 nm, while the pit diameter enlarges rapidly at first up to 15  $\mu\text{m}$  and then slows down. Such quantitative data is not only useful for kinetic studies of the degradation but also allows the influence of the pits on the change of the surface appearance, such as gloss loss, to be assessed.

The phase images in tapping mode AFM can provide valuable information on surface microstructure changes, which are not visible in topographic images. This capability particularly benefits the characterization of the degraded coating surface that is rough and pitted. In *Figure 6*, the surface microstructure of an epoxy (E1000) film is shown before and after exposure to outdoor conditions in the Washington D.C. area during summer. Initially, the surface of the fresh epoxy film is smooth and there are no visible features in the phase image. After one month of exposure, pitting is observed. The diameters of the pits range from a few nanometers to hundreds of nanometers, but the depths are only a few nanometers. The phase images clearly show two phase heterogeneous structures with bright nodules, especially inside the pits. While these nodules are similar to those observed on the interface side and the bulk of the E1000 film (*Figures 1B and 2*), they are more irregular in their sizes and shapes. The nodules inside the pits appear larger than those in the relatively smooth area. Our extensive AFM results of degraded epoxy samples indicate that the heterogeneous structure of this type of epoxy coating is not limited at the film/substrate interface but also through the bulk of the sample. The surface rearrangement or/and degradation is believed to occur when the sample is exposed to the environment. The low surface-free energy layer on the top of the film probably is degraded or rearranged, exposing the bulk microstructure of the epoxy films shown in *Figure 2*. After two months of exposure (*Figure 6C*), the surface becomes rougher, and the larger pits appear. When a pit is closely examined, irregular nodular structure is observed. Some nodules are as large as a hundred nanometers. This information can only be revealed clearly by the phase images, not by topographic images.

Another advantage of using tapping mode AFM for the study of coating degradation is its capability of generating force curves while the sample is being imaged. In this operation, the AFM probe tip is first lowered into contact with the sample, then indented into the surface, and finally lifted off the sample surface. Concurrently, a meas-

urement of the probe tip deflection as a function of the vertical displacement of the piezo scanner is produced. A plot of this tip deflection signal is called a force-displacement curve or force curve. Generally, the mechanically different regions can be identified from the slope and shape of the repulsive or contact portion of the force curves obtained by the appropriate probe tips. Because the degraded sample surfaces are often highly heterogeneous at a submicron scale, force curve can be combined with phase imaging to determine mechanical, viscoelastic, and/or adhesive differences between the different regions of the coating surfaces. In this article, we demonstrate the use of this technique for obtaining heterogeneity information in degraded polyester films.

Our previous study has shown that the base-catalyzed hydrolysis of polyester is a heterogeneous process, involving the formation of pits that increase in number and size with exposure time.<sup>15</sup> In *Figure 7*, AFM images of an area around a pit are shown along with the force curves of the regions inside and outside the pit for a polyester film exposed to 3 mol/l NaOH solution for 28 days. The phase contrast appears darker inside the pit with respect to the surrounding areas. However, large patches with brighter phase contrast also appear in the area above and to the left of the pit. Compared to the regular nodular structures of the unexposed polyester (not shown here), the phase image in *Figure 7A* indicates that the microstructure of the exposed polyester has substantially changed and the pitted region has different mechanical and/or chemical properties from the unpitted area. Although absolute values for the elasticity and the adhesion force are still difficult to obtain, the mechanical behavior in the different regions of the same sample can be compared from the AFM force curves. The characteristics of the force curve in the unpitted region (portion (b) of *Figure 7B*) shows that the materials in this region are stiff and hard for the utilized tip to penetrate. For the area inside the pit, however, a greater pull-off force and a larger hysteresis between the loading and unloading curves are observed of *Figure 7B* (a). The force curve in *Figure 7B* (a) shows that the AFM tip initially

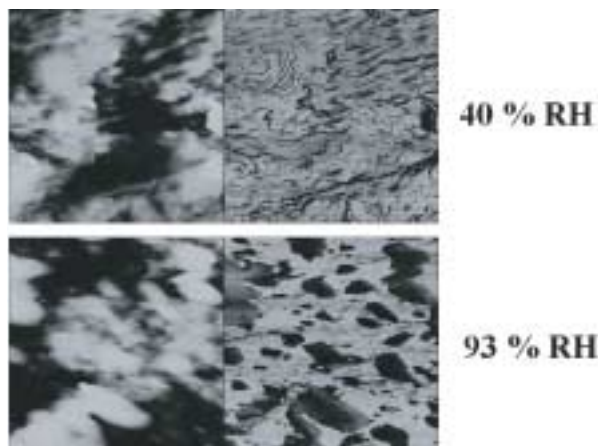


Figure 8—AFM images of the fractured surface of PS-b-PEO bulk specimen at different RHs. The scan size is  $3 \times 3 \mu\text{m}$ , and contrast variations from black to white are 150 nm for the height image (left) and  $90^\circ$  for the phase image (right).

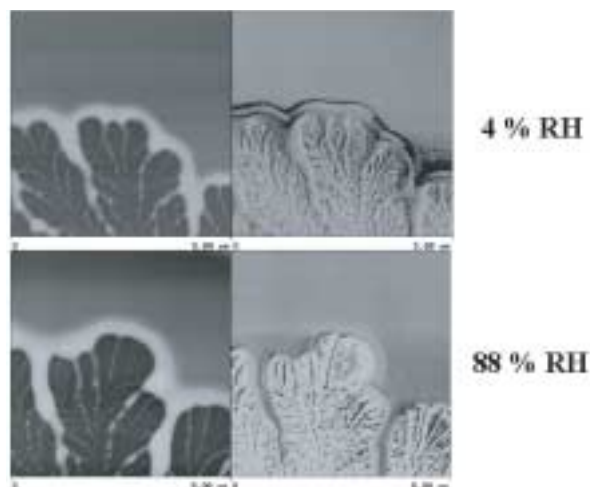


Figure 9—AFM images at different RH levels of PS-PAA dewetting patterns. The scan size is  $5 \times 5 \mu\text{m}$ , and contrast variations from black to white are 150 nm for the height image (left) and  $90^\circ$  for the phase image (right).

penetrates into the sample for about 100 nm, and then it begins to encounter a stiffer material that makes it hard to penetrate further. The results suggested that, in the dark phased region inside the pit, a compliant layer might cover the rigid materials of the polyester. It is believed that some degraded products are in this layer, and they seem more adhesive or plastic than those undegraded materials in the unspitted region. In combination with force curves, therefore, the phase images can provide more detailed information on the heterogeneity of the coating degradation.

### Characterizing Surface Chemical Heterogeneity of Polymer Coatings with AFM

The ability to probe chemical heterogeneity with nanometer scale resolution is essential to developing a molecular-level understanding of a variety of phenomena occurring at coating surfaces, such as adhesion, friction, and degradation. However, the ability to identify and map the surface chemical heterogeneity has remained an unfulfilled opportunity in the field of AFM. Phase imaging in tapping mode AFM can provide important information for the surface heterogeneity from the differences in energy dissipation of the different domains; however, it is hard to differentiate the contributions of their mechanical and chemical properties. Chemical force microscopy (CFM)<sup>17,18</sup> is a successful technique to enhance the chemical sensitivity of AFM through modification of the AFM tip with controlled functional groups. The key to the success of this technique is ensuring that interactions be-

tween the modified tip and the sample surface are dominated by the chemical species on the surface of the tip and the sample surface studied. Because capillary forces resulting from the adsorption of ambient water onto the sample surface are usually one to two orders of magnitude higher than specific chemical interactions, CFM has usually been conducted in liquid instead of air to eliminate capillary effects. Most CFM research has been performed on patterned self-assembled monolayers (SAM), where the hydrophilic and hydrophobic domains are well defined and well organized. For real world materials, such as polymer blends and coatings, solvent is not a desirable medium because it can cause irreversible changes to the sample.

Recently, a well controlled humidity system has been developed to enhance the sensitivity of AFM in characterizing surface chemical heterogeneity. The relative humidity in the sample-tip environmental chamber can be controlled from nearly 0 up to 95% RH at room temperature. Our results have shown that the image contrast between hydrophilic and hydrophobic regions of a surface is substantially increased in elevated relative humidity environments.<sup>19</sup> One example is illustrated in *Figure 8* for a model coating system—a block copolymer of polystyrene-*b*-polyethylene (PS-*b*-PEO)—in which images are shown for similar locations on the fractured surface of the PS-*b*-PEO sample at different RHs. Compared to that at lower humidity (40% RH), the phase image at a higher humidity (93% RH) exhibits a dramatic increase in the phase contrast between different domains, and a large area of dark-phased domains is observed. The light regions in the phase image are believed to be PS regions, which is the hydrophobic component. The dark domains are believed to be the highly hydrophilic and water soluble PEO regions. At high humidity, these regions are swollen and surface rearrangement has taken place. These results indicate that the PEO domains are softened at the elevated humidity, and the interactions between the tip and PEO domains are enhanced by the adsorbed moisture. Thus, the surface regions with different chemical properties can be distinguished by AFM phase imaging. Similar results are observed in *Figure 9* for a bilayer film of polystyrene and poly(acrylic acid) (PS-PAA), where the flat region outside the fingering pattern is the hydrophilic PAA layer, and the lower flat area inside the pattern was the hydrophobic PS-rich region.<sup>24</sup> Studies are underway on use of chemically modified tips combined with the humidity chamber for chemical imaging of polymeric coatings.

### Characterizing Nanomechanical Properties with Nanoindentation

Mechanical behaviors such as elastic modulus and hardness can be obtained by AFM through multiple individual force-displacement curves. However, quantitative analyses of AFM data are complicated by the uncertainties relating the probe spring constant and tip geometry, hysteresis and creep of the piezoelectric scanners, and instrument compliance and system electronics corrections.<sup>21,31</sup> Instrumented indentation or nanoindentation can overcome some of these problems. Recent developments in adding dynamical oscillation for improved sensitivity to the penetration depth, and a higher level of test automation and data ac-

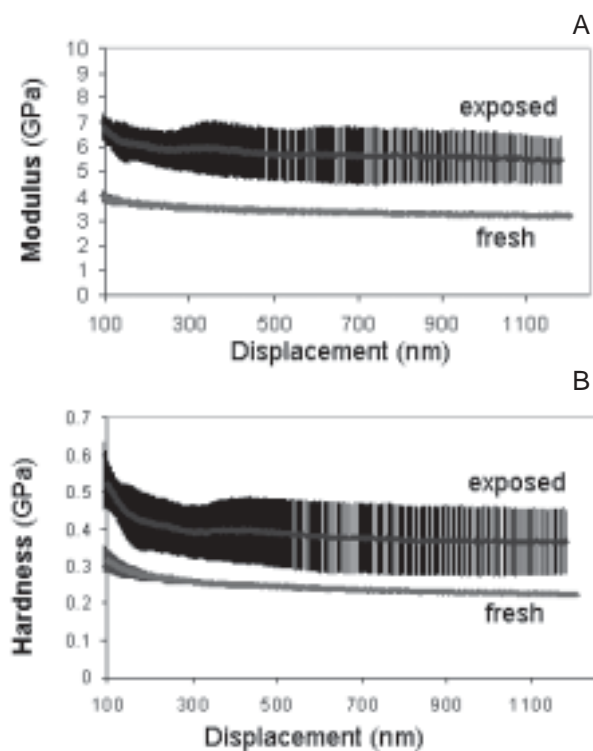


Figure 10—Modulus and hardness as a function of indentation depth for an epoxy coating film before (A) and after (B) exposure to outdoor environments in Washington D.C. area for 220 days. Error bars represent the standard deviation.

quisition have increased the application of nanoindentation for studying the mechanical properties of polymer coatings.<sup>21,22</sup> Figure 10 shows the evolution of modulus and hardness versus indentation depth for an epoxy (E1000) coating film before and after exposure to outdoor environments in the Washington D.C. area for 220 days. Each data point is the mean with error bars representing the standard deviation calculated from 10 indents at different locations. Significant increases in both modulus and hardness are clearly observed for the exposed sample over the whole range of indentation depth even though the standard deviations of modulus and hardness of the exposed sample are large. Our extensive FTIR studies<sup>7</sup> have shown that photodegradation of the epoxy coating involves reactions such as oxidation, chain scission, and crosslinking. These chemical reactions may cause the observed mechanical changes of the film, at least for the near-surface region. The corresponding AFM study revealed that pits, cracks, ablation, degraded products, and dust particles dramatically increase the roughness of the sample surface. The increased roughness and the nonuniform morphology could be a reason for the large standard deviations observed in modulus and hardness of the exposed samples. However, the mechanical heterogeneity in different regions of the degraded sample surface could possibly be another reason. The sensitivity to the heterogeneity of the different regions is affected by the indenter geometry and contact area. The Berkovich indentation tip used in this study has a radius of curvature of approximately 100 nm, and thus, might be more sensitive to local mechanical variations. Regardless, the results have clearly demonstrated the effects of the photodegradation on the surface mechanical properties of the epoxy coating.

The nanoindentation instrument has also been widely used to study the scratch and mar resistance of polymer coatings. Three main types of scratch damage are normally identified: elastic-plastic deformation, regularly fractured scratches, and irregularly fractured scratches.<sup>23</sup> Transitions between these types of scratch damage with increasing load have been used to define so-called critical load ( $L_c$ ) values.<sup>23,32</sup> Additionally, the characteristics of the residual deformation pattern, particularly the shape of the ruptures at loads above  $L_c$  can provide additional information on the material behavior.<sup>32</sup> However,  $L_c$  is strongly dependent on indenter geometry and other test parameters, leading to poor reproducibility and misleading results. Time-dependent properties of a coating surface, such as viscoplastic deformation and viscoelastic relaxation, can also be obtained by the examination of the scratch width resulting from the various scratch velocities at a constant load and the measurement of the residual scratch depth after a specific period of time, respectively. The capability of lateral force measurement of the nanoindentation instrument also allows for the determination of friction force and friction coefficient. In Figure 11, laser scanning confocal microscopy images of the fracture patterns are shown for three different materials: an amine-cured epoxy, PMMA, and high crystalline PP. The moduli of these three samples obtained from nanoindentation tests are  $3.17 \pm 0.22$  GPa for epoxy,  $5.11 \pm 0.08$  GPa for PMMA, and  $2.04 \pm 0.04$  GPa for PP. The scratch tests were performed using an increasing load from 0–18 mN at a

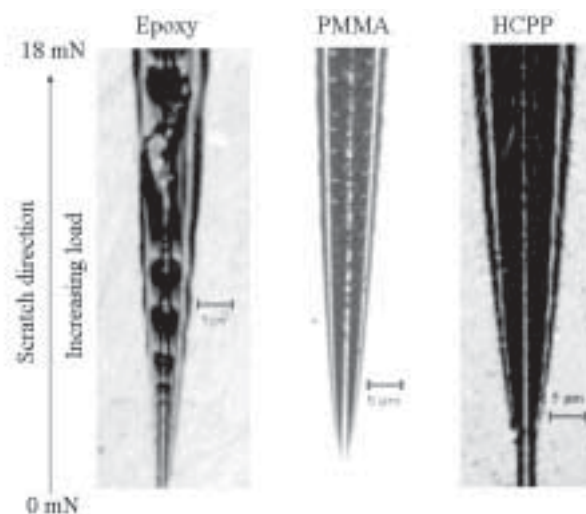


Figure 11—Laser scanning confocal micrographs of the scratch deformation for three different materials: epoxy, PMMA, and PP. The progressive-load scratch test was performed using a diamond tip with a 1- $\mu\text{m}$  tip radius and a 90° cone angle. The scratch speed was 250  $\mu\text{m}/\text{sec}$ .

constant scratch velocity of 250  $\mu\text{m}/\text{sec}$  using a rounded 90° conic indenter with a tip radius of approximately 1  $\mu\text{m}$ . As can be seen, the characteristics of the three deformation patterns are substantially different. An irregular fractured pattern is shown in epoxy, a concave deformation pattern is observed in PMMA, and a convex deformation pattern in PP.<sup>32</sup> Among the three materials, epoxy and PMMA are relatively brittle and PP is more compliant. The ability of the thermoset epoxy to deform under tensile or shearing stresses is limited by its crosslinked structure compared to the two thermoplastic polymers. Also, epoxy is completely amorphous, while PMMA may perhaps have low levels of crystallinity and PP has a much higher level of crystallinity. These differences in structure and properties likely affect the observed differences in scratch damage. Because the scratch morphology and the scratch resistance affect the appearance performance of coatings, developing an improved understanding of the relationships between scratch mechanisms and the material structure and properties will facilitate material selection and performance improvement.

## CONCLUSIONS

The application of tapping mode AFM to studies of surface microstructure and degradation of polymer coatings has been demonstrated. The results have shown that tapping mode AFM is a powerful technique for coating characterization that can provide direct spatial mapping of surface topography along with nanoscale microstructural information that reflects the property differences of heterogeneous coating materials. An environmental chamber was used to control the relative humidity of the imaging environment, resulting in enhanced sensitivity of tapping mode AFM on various chemical properties. Thus, the surface chemical heterogeneity of polymers can be distinguished by AFM when the tip and sample environment is controlled using high

humidity. The application of nanoindentation to studies of surface mechanical properties, such as modulus, hardness, and scratch resistance of coating materials has also been shown. The results indicate that nanoindentation is an important tool for studying surface mechanical changes of coatings during degradation. The capability to capture the mechanical properties as a function of indentation depth with nanometer scale resolution in depth provides valuable information about the process of coating degradation. The additional scratch capability of the nanoindentation device allows for studies on surface mechanical properties related to appearance. It is believed that the characterization of coating surface with these nanoscale techniques would provide a better understanding of degradation mechanisms, thus improving the service life performance of polymer coatings.

## References

- (1) Thomas, H.R. and Omalley, J.J., "Surface Studies on Multicomponent Polymer Systems by X-Ray Photoelectron-Spectroscopy-Polystyrene-Poly(ethylene oxide) Diblock Copolymers," *Macromolecules*, 12, 323-329 (1979).
- (2) Lee, W.K., Cho, W.J., Ha, C.S., Takahara, A., and Kajiyama, T., "Surface Enrichment of The Solution-Cast Poly(methyl methacrylate) Poly(vinyl acetate) Blends," *Polymer*, 36, 1229-1234 (1995).
- (3) Ebbens, S.J. and Badyal, J.P.S., "Surface Enrichment of Fluorochemical-Doped Polypropylene Films," *Langmuir*, 17, 4050-4055 (2001).
- (4) Chen, X., McGurk, S.L., Davies, M.C., Roberts, C.J., Shakesheff, K.M., Tendler, S.J., and Williams, P.M., "Chemical and Morphological Analysis of Surface Enrichment in a Biodegradable Polymer Blend by Phase-Detection Imaging Atomic Force Microscopy," *Macromolecules*, 31, 2278-2283 (1998).
- (5) Bascom, W.D., *J. Adhesion*, 2, 168 (1970).
- (6) Corti, H., Fernandez-Prini, R., and Gomez, D., "Protective Organic Coatings-Membrane-Properties and Performance," *Prog. Org. Coat.*, 10, 5-33 (1982).
- (7) Gu, X., Nguyen, T., and Martin, J.W. (unpublished results).
- (8) Delobelle, P., Guillot, L., Dubois, C., Perreux, D., and Monney, L., "Photo-Oxidation Effects on Mechanical Properties of Epoxy Matrixes: Young's Modulus and Hardness Analyses By Nano-indentation," *Polym. Degrad. Stab.*, 77, 465-475 (2002).
- (9) Cleveland, J.P., Anczykowski, B., Schmid, A.E., and Elings, V.B., "Energy Dissipation in Tapping-Mode Atomic Force Microscopy," *Appl. Phys. Lett.* 72, 2613-2615 (1998).
- (10) Magonov, S.N. and Reneker, D.H., "Characterization of Polymer Surfaces with Atomic Force Microscopy," *Annu. Rev. Mater. Sci.*, 27, 175-222 (1997).
- (11) Magonov, S.N., Elings V., and Whangbo, M.H., "Phase Imaging and Stiffness in Tapping-Mode Atomic Force Microscopy," *Surf. Sci.*, 375, L385-L391 (1997).
- (12) Bar, G., Thomann Y., and Whangbo, M.H., "Characterization of Morphologies and Nanostructures of Blends of Poly(styrene) Block-Poly(ethane-co-but-1-ene)-Block-Poly(styrene) with Isotactic and Atactic Polypropylenes by Tapping-Mode Atomic Force Microscopy," *Langmuir*, 14, 1219-1226 (1998).
- (13) Raghavan, D., Gu, X., Nguyen, T., VanLandingham, M.R., and Karim, A., "Mapping Polymer Heterogeneity Using Atomic Force Microscopy Phase Imaging and Nanoscale Indentation," *Macromolecules*, 33, 2573-2583 (2000).
- (14) Raghavan, D., Gu, X., Nguyen, T., and VanLandingham, M.R., "Characterization of Chemical Heterogeneity in Polymer System Using Hydrolysis and Tapping-Mode Atomic Force Microscopy," *J. Polym. Sci. Polym. Phys.*, 39, 1460-1470 (2001).
- (15) Gu, X., Raghavan, D., Nguyen, T., and VanLandingham, M.R., "Characterization of Polyester Degradation Using Tapping Mode Atomic Force Microscopy: Exposure to Alkaline Solution at Room Temperature," *Polym. Degrad. Stab.*, 74, 139-149 (2001).
- (16) Bar, G., Thomann, Y., Brandsch, R., and Cantow, H.-J., "Factors affecting the Height and Phase Images in Tapping Mode Atomic Force Microscopy. Study of Phase-Separated Polymer Blends of Poly(ethane-co-styrene) and Poly(2,6-dimethyl-1,4-phenylene Oxide)," *Langmuir*, 13, 3807 (1997).
- (17) Frisbie, C.D., Rozsnyai, L.F., Noy, A., Wrighton, M.S., and Lieber, C.M., "Functional-Group Imaging by Chemical Force Microscopy," *Science*, 265, 2071-2074 (1994).
- (18) Noy, A., Vezenov, D.V., and Lieber, C.M., "Chemical Force Microscopy," *Annu. Rev. Mater. Sci.* 27, 381-421 (1997).
- (19) Martin, J.W., Embree E., and VanLandingham M.R., U.S. Patent, U.S. 6.490.913 B1 (2002).
- (20) Gu, X., VanLandingham, M.R., Fasolka, M., Martin, J.W., Jean, Y.C., and Nguyen, T., "Enhancing Sensitivity of Atomic Force Microscopy for Characterizing Surface Chemical Heterogeneity," in the Proc. 26th Adhesion Society Meeting, 185-187, 2003.
- (21) Chong K.P., VanLandingham M.R., and Sung L., "Advances in Materials and Mechanics," in the Proc. International Conference on Advances in Building Technology, 3-16, 2002.
- (22) VanLandingham, M.R., Chang, N.K., White, C.C., and Chang S.H., "Viscoelastic Characterization of Polymers Using Instrumented Indentation-I. Quasi-static Testing," *J. Mat. Res.*, submitted for publication (2003).
- (23) Jardret, V., Lucas, B.N., and Oliver, W., "Scratch Durability of Automotive Clear Coatings: A Quantitative, Reliable and Robust Methodology," *JOURNAL OF COATINGS TECHNOLOGY*, 72, No. 907, 79 (2000).
- (24) Gu, X., Raghavan, D., Douglas, J., and Karim, A., "Hole-Growth Instability in the Dewetting of Unstable Viscous Polymer Films," *J. Polym. Sci. Polym. Phys.* 40, 2825-2832 (2002).
- (25) VanLandingham, M.R., Camara, R., and Villarrubia J.S., "Measuring Tip Shape for Instrumented Indentation Using Atomic Force Microscopy," *J. Mat. Res.*, submitted for publication (2003).
- (26) Nguyen, T., Gu, X., VanLandingham, M.R., Giraud, M., Dutruc-Rosset, R., Ryntz, R., and Nguyen, D., "Characterization of Coating System Interphases with Phase Imaging AFM," in the Proc. Adhesion Society Meeting, 68-70, 2001.
- (27) Gu, X., Raghavan, D., Ho, D.L., Sung, L., VanLandingham, M.R., and Nguyen, T., "Nanocharacterization of Surface and Interface of Different Epoxy Networks," *Mat. Res. Symp. Proc.*, 710, DD10.9.1-DD10.9.6 (2001).
- (28) Kalivianakis, P. and Jungnickel, B.J., "Crystallization-Induced Composition Inhomogeneities in PVDF/PMMA Blends," *J. Polym. Sci. Polym. Phys.*, 36, 2923-2930 (1998).
- (29) Briber, R.M. and Khoury, F., "The Phase Diagram and Morphology of Blends of Poly(vinylidene fluoride) and Poly(ethyl acrylate)," *Polymer*, 28, 38-42 (1987).
- (30) Gu, X., Sung, L., Ho, D.L., Michaels, C.A., Nguyen, D., Jean, Y.C., and Nguyen, T., "Surface and Interface Properties of PVDF/Acrylic Copolymer Blends Before and After UV Exposure," in the Proc. International Coating Technology Conference, 2002.
- (31) VanLandingham, M.R., Villarrubia J.S., Guthrie, W.F., and Meyers, G.F., "Nanoindentation of Polymers: An Overview," *Macromolecules Symposia*, 167, 15-43 (2001).
- (32) Krupicka, A., Johansson, M., and Hult, A., "Mechanical Surface Characterization: A Promising Procedure to Screen Organic Coatings," *JOURNAL OF COATINGS TECHNOLOGY*, 75, No. 939, 19 (2003).